IEEE Photonics Journal
An IEEE Photonics Society Publication

Open Access

The Impact of LED Correlated Color Temperature on Visual Performance Under Mesopic Conditions

Volume 9, Number 6, December 2017

Lili Dong
Li Qin
Wenhai Xu
Lidong Zhang

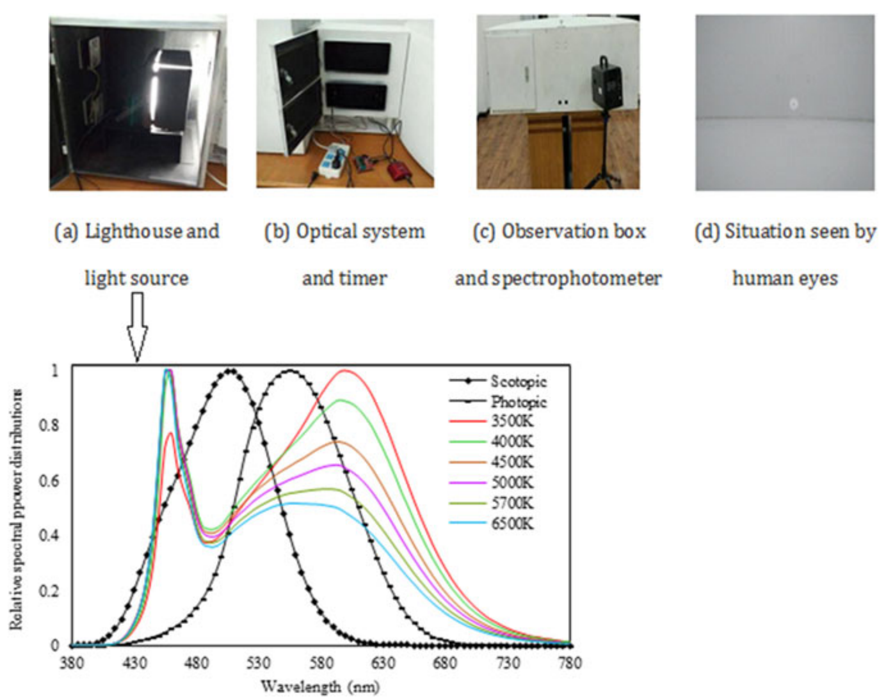

DOI: 10.1109/JPHOT.2017.2760257
1943-0655

The Impact of LED Correlated Color Temperature on Visual Performance Under Mesopic Conditions

Lili Dong,[1] **Li Qin**,[1] **Wenhai Xu,**[1] **and Lidong Zhang**[2]

[1]School of Information Science and Technology, Dalian Maritime University, Dalian 116026, China
[2]High Grade Highway Construction Authority of Jilin Province, Jilin 130012, China

DOI:10.1109/JPHOT.2017.2760257

Manuscript received September 19, 2017; revised October 3, 2017; accepted October 3, 2017. Date of publication October 6, 2017; date of current version November 2, 2017. Corresponding author: Li Qin (e-mail: 1073015583@qq.com).

Abstract: The aim of this study was to investigate the impact of correlated color temperature (CCT) of LED light source on human vision performance in mesopic region. First, six CCTs (3500, 4000, 4500, 5000, 5700, and 6500 K) were assessed using mesopic photometry model MES-2. The calculation results indicated that the mesopic luminance had a positive correlation with CCT. Then, reaction time experiment was conducted in an experimental box designed to simulate the mesopic application environments. Ten observers of different ages and gender participated to make response after target appears under different lighting conditions. Experiment results showed that reaction time had a negative correlation with CCT, which is coherent with that the mesopic luminance increased with the increasing of CCT.

Index Terms: Mesopic vision, correlated color temperature, reaction time, visual performances.

1. Introduction

The dynamic range of human visual system covers a wide luminance from 10^{-3} cd/m^2 to 10^6 cd/m^2. And according to the change of environment luminance, vision may be classified simply as of three types [1]: photopic vision, scotopic vision, and mesopic vision.

Photopic vision is extended from the upper luminance of the mesopic vision up to the maximum visible stimulus. While scotopic vision is generally believed to extend from the minimum visible stimulus up to about 0.001 cd/m^2 [1], which can be considered as the lower limit of the mesopic region. The upper luminance limit of mesopic region cannot be precisely defined, as it is dependent on several factors, including the size and position of the visual object in the field of view. The CIE definition for the border between mesopic and photopic luminance region is ‘at least several cd/m^2’ [2]. Mesopic lighting applications are of substantial practical interests as they include road and street lighting, outdoor lighting, tunnel lighting, night-time traffic conditions and many other applications.

Reasonable selection of lighting source is crucial to ensure the safety and energy-saving of lighting system. During the last decade, lighting technology based on LED has advanced rapidly and is paving the way for application of LED lighting [2]. LED has been widely used in many lighting fields such as road and street lighting, emergency escape lighting, marine lighting, night-time lighting, and many other fields (most of them belong to mesopic vision) because of its advantages (LED requires less maintenance, provides high brightness to drivers, has high color rendering index and provides better safety perception to drivers [3], [4]). However the correlated color temperature (CCT) of LED varies from 2700 K to 6500 K along with the color changing from warm white into cold white. Thus different CCTs of LED may have different effects on human visual performance. The purpose of this research is to investigate the effect of LED CCT on visual performance under mesopic environments.

2. Mesopic Vision Theory

The development of mesopic photometry has raised interest in the international lighting community for several decades [5]. Unlike the photopic (which relies on the photopic spectral luminous efficiency function $V(\lambda)$, established by Commission Internationale de L'Eclairage (CIE) in 1924 [6]), and scotopic (which can be described by the $V'(\lambda)$ function, established by the CIE in 1951) spectral luminous efficiency functions, it is not possible to describe mesopic spectral luminous efficiency with a single function since the interaction between cones and rods differs with light levels.

In the mesopic region there have been two methods to establish the mesopic sensitivity function: brightness matching and visual performance-based approaches [7]. The early works on mesopic luminous efficiency were mostly based on brightness matching. Walters and Wright [8], and Kinney [9] used heterochromatic brightness matching to derive mesopic luminous efficiency functions. Several field sizes, luminance levels, and eccentricities were used in their study. In 1989, the CIE introduced five mesopic photometry models based on brightness matching [10]. They described the shift of spectral sensitivity towards shorter wavelengths with the decrease of light levels in the mesopic region. A CIE report in 2001 [11] updated the earlier report and added a new mesopic photometry model based on heterochromatic brightness matching for 10° fields.

Another main method for obtaining luminous efficiency functions is visual performance-based approach. In recent years, the CIE has recognized the merit of this approach and it has been a topic of study. Rea and colleagues [12] presented the X-model as a unified system for photometry. It is based on the earlier reaction time experiments by He and colleagues [13], [14]. The mesopic luminous efficiency $V_{mes}(\lambda)$ in X-model is a linear transition between the scotopic $V'(\lambda)$ and the photopic $V(\lambda)$ functions, as follows,

$$V_{mes}(\lambda) = X\,V(\lambda) + (1 - X)V'(\lambda) \tag{1}$$

$$X = \frac{1}{0.599}L_m - \frac{0.001}{0.599}$$

Where the parameter X characterizes the proportion of the photopic luminous efficiency at any luminance level. X = 1 represents photopic conditions, while X = 0 represents scotopic conditions. And the valid luminance in X-model is between 0.001 cd/m^2 and 0.6 cd/m^2.

MOVE (Mesopic Optimization of Visual Efficiency) [15] was proposed on the basis of experimental work carried out in several test locations. In experiments, reaction time for many coloured targets, detection threshold, and recognition threshold were used as the visual tasks. There were 109 observers participated in the experiments and all experiments were based on a common set of parameter values. The form of MOVE model is as below,

$$M(x)V_{MOVE}(\lambda) = xV(\lambda) + (1 - x)V'(\lambda) \tag{2}$$

M(x) is a normalized factor such that $V_{MOVE}(\lambda)$ attains a maximum value of 1. The parameter x determines the proportions of the photopic and scotopic functions.

As can be seen above, the X- and MOVE-models have similar forms and the major difference between them results from the choice of the transition point between mesopic and photopic regions. The upper luminance limit (0.6 cd/m^2) of the X-model is believed too low, while the upper limit (10 cd/m^2) of the MOVE-model is considered too high.

So CIE published a system for visual performance-based mesopic photometry [16] in 2010, which is combination of the MOVE and the Unified System of photometry derived from the work of He *et al*. [13], [14]. This model is known as MES-2 model, and its upper luminance level is at 5 cd/m^2

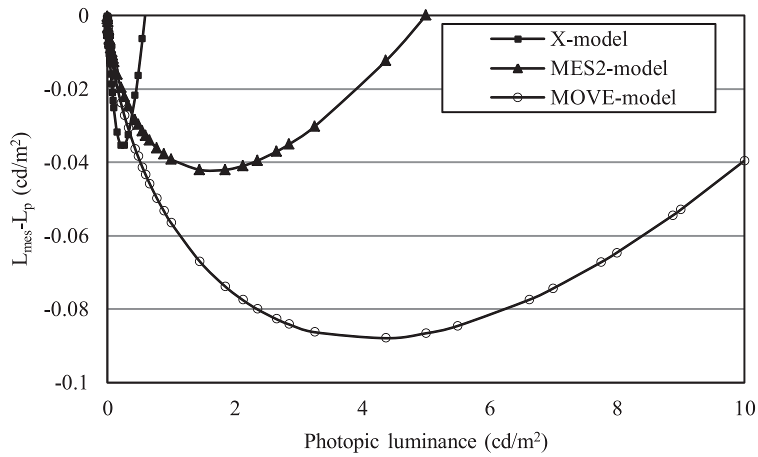

Fig. 1. The curve of difference between mesopic and photopic luminance (S/P of light source is 0.65).

(this limit is sufficiently to cover all practical street, road lighting levels under varying weather conditions), and lower luminance level is at 0.005 cd/m^2. The model is derived from the same experimental data as the MOVE-model, and it describes spectral luminous efficiency, $V_{mes}(\lambda)$, in the mesopic region as a linear combination of the photopic spectral luminous efficiency function, $V(\lambda)$, and the scotopic spectral luminous efficiency function, $V'(\lambda)$, and establishes a gradual transition between these two functions. The model is of the form:

$$M(m_2)V_{mes2}(\lambda) = m_2 V(\lambda) + (1 - m_2)V'(\lambda) \tag{3}$$

and

$$L_{mes,n} = \frac{m_{2,n-1}L_p + (1 - m_{2,n-1})L_s V'(\lambda_0)}{m_{2,n-1} + (1 - m_{2,n-1})V'(\lambda_0)} \qquad m_{2,0} = 0.5 \tag{4}$$

and

$$m_{2,n} = 0.3334\log_{10}L_{mes,n} + 0.767 \quad 0 \leq m_{2,n} \leq 1 \tag{5}$$

Where $M(m_2)$ is a normalizing function so that $V_{mes2}(\lambda)$ attains a maximum value of 1, m_2 is a coefficient dependent on the visual adaptation conditions, L_{mes} is the mesopic luminance, L_p is the photopic luminance, L_s is the scotopic luminance, and $V'(\lambda_0) = 683/1700$ is the value of scotopic spectral function $V'(\lambda)$ at 555 nm, and n is an iteration step.

In order to compare the characteristics of three mesopic visual models, two light sources (the one's $S/P = 0.65 < 1$, the other one's $S/P = 1.65 > 1$, S/P value of light sources can be calculated by (6)) are selected to compare the mesopic luminance difference values calculated by three models.

Figs. 1 and 2 plot the difference value curve between mesopic luminance and photopic luminance ($L_{mes} - L_p$) varies with the photopic luminance when S/P value of light source is 0.65 and S/P value of light source is 1.65, respectively.

It should be clearly seen from Figs. 1 and 2 that the adaptive luminance scope of three models is different. Furthermore, for the same photopic luminance of light source, the mesopic luminance calculated by three models is different. And for X-model, the mesopic luminance is equivalent to the photopic luminance at 0.6 cd/m^2 (the upper luminance limit). For MES2-model, the mesopic luminance is also equivalent to the photopic luminance at 5 cd/m^2 (the upper luminance limit). While for MOVE model, the mesopic luminance is not equivalent to the photopic luminance at 10 cd/m^2 (the upper luminance limit). It indicates that X- and MES2- models have a high accuracy at high luminance region, and the MOVE-model has a low accuracy at high luminance region.

From Fig. 1, we can see that mesopic luminance is less than photopic luminance when light source's S/P value is less than 1, which means the light appears to be less bright than the measured luminance (S/P value of High Pressure Sodium (HPS) is always less than 1). While in Fig. 2, mesopic luminance is greater than photopic luminance when light source's S/P value is greater than 1, which

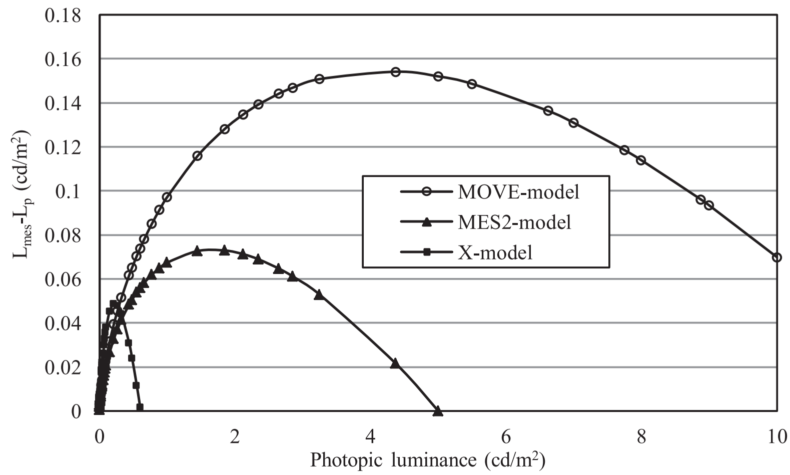

Fig. 2. The curve of difference between mesopic and photopic luminance (S/P of light source is 1.65).

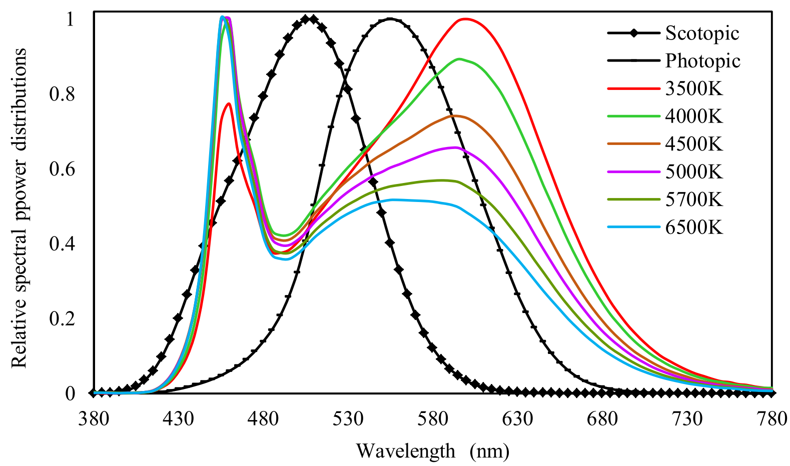

Fig. 3. Results of spectra distribution.

means the light appears to be brighter than the measured luminance (S/P value of LEDs are always greater than 1). Thus, the mesopic luminance calculated by the same mesopic visual model can be varied with the change of S/P values.

The upper luminance limit (0.6 cd/m^2) of the X-model is believed too low, while MOVE-model has a low accuracy at high luminance region. So CIE recommended MES2-model as the mesopic photometry model. This research adopted the MES-2 model to discuss the impact of LED CCT on the human visual performance, and then used the reaction time experiment to test the effect.

3. The Impact of LED CCT on the Human Visual Luminance

3.1 The Spectral Power Distribution (SPD) of Light Source

Currently CCTs of LED available in the market are 2700 k, 3000 k, 3500 k, 4000 k, 4500 k, 5000 k, 5700 k and 6500 k. The six CCTs (3500 k, 4000 k, 4500 k, 5000 k, 5700 k, and 6500 k) were chosen in this research. The LED light source spectrum was measured by the spectrophotometer Konica-Minolta CS 2000. The relative spectral distributions of different types of LEDs, photopic, and scotopic spectral luminous efficiency function are shown in Fig. 3.

From the Fig. 3, we can see that the LED spectrum was characterized by a wide spectrum double-peak pattern.

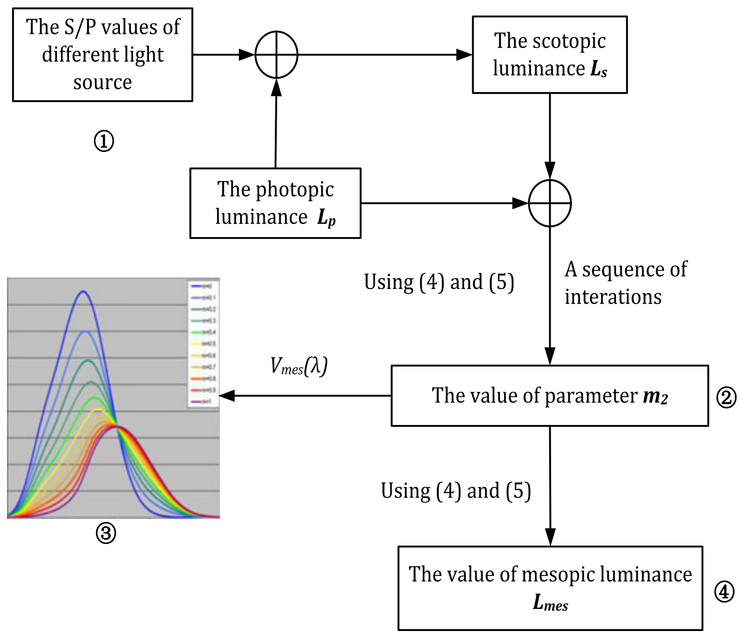

Fig. 4. Calculation process.

3.2 The Impact of Light Source CCT on $V_{mes}(\lambda)$ and Mesopic Luminance

We can see from (3) that mesopic spectral luminous efficiency function $V_{mes2}(\lambda)$ is determined by the parameter m_2 in MES-2 model. Equations (4) and (5) indicate that the value of m_2, the mesopic luminance L_{mes}, the photopic luminance L_p and scotopic luminance L_s are related. The photopic luminance can be measured by the luminance meter, which is corrected by the photopic spectral luminous efficiency function V(λ). The scotopic luminance L_s can be calculated based on the L_p and the S/P-ratio of light source. And the S/P is ratio of scotopic to photopic luminous output.

In order to calculate the $V_{mes2}(\lambda)$ of different CCTs with certain background luminance L_p, and calculate mesopic luminance L_{mes} of different CCTs in different background luminances L_p, the calculation process can be represented by Fig. 4.

Step 1: the calculation of S/P-ratio of light source [17].

The S/P value is scotopic to photopic luminous flux ratios of light sources. And the S/P value of light source can be calculated by (6).

$$s/p = \frac{\Phi_s}{\Phi_p} = \frac{1700 \int_{380}^{780} L(\lambda) V'(\lambda) d\lambda}{683 \int_{380}^{780} L(\lambda) V(\lambda) d\lambda} \tag{6}$$

where $V'(\lambda)$ is scotopic spectral luminous efficiency function, $V(\lambda)$ is photopic spectral luminous efficiency function, and the $L(\lambda)$ is the spectral power distribution (SPD) of the light source. The S/P-ratios of the above mentioned six LED sources are shown in Table 1.

It can be seen from Table 1 that the S/P-ratios of LEDs are all greater than 1.0. And S/P-ratios are clearly increased with increasing CCT from 3500 k to 6500 k.

Step 2: the calculation of parameter m_2.

The values of m_2 can be calculated based on the photopic luminance, scotopic luminance, (4) and (5).

Table 2 lists the value of m_2 for the background luminance at 1 cd/m^2, 2 cd/m^2, 3 cd/m^2 and 4 cd/m^2 of each CCT.

It can be seen from Table 2 that the value of m_2 is increased with increasing S/P-ratios from 1.598 to 2.269 when the photopic luminance keeps invariant. And when the S/P-ratio is unchanged

TABLE 1
The S/P Value of Six Light Sources

Light source	S/P-ratio
3500-k LED	1.598
4000-k LED	1.817
4500-k LED	1.977
5000-k LED	2.074
5700-k LED	2.178
6500-k LED	2.269

TABLE 2
The Values of m_2 for LEDs Under Different Photopic Luminances

m_2 / S/P-ratio	Photopic Luminance (cd/m^2)			
	1	2	3	4
1.598 (3500K)	0.7757	0.8721	0.9286	0.9688
1.817 (4000K)	0.7787	0.8737	0.9295	0.9692
1.977 (4500K)	0.7807	0.8749	0.9302	0.9695
2.074 (5000K)	0.7819	0.8755	0.9305	0.9696
2.178 (5700K)	0.7831	0.8762	0.9309	0.9698
2.269 (6500K)	0.7842	0.8769	0.9313	0.9700

(which means the CCT is the same), the values of m_2 are increased with increasing from photopic luminance from 1 cd/m^2 to 4 cd/m^2.

Step 3: description of $V_{mes2}(\lambda)$.

In accordance with SI definition of candela, luminous efficiency at 555 nm is always 683 lm/W. Thus, in the mesopic region, the maximum spectral luminous efficiency can be calculated by (7).

$$K_m = \frac{683 lm \cdot W^{-1}}{V_{mes2}(\lambda = 555 \text{ nm})} \tag{7}$$

where $V_{mes2}(\lambda = 555\,\text{nm})$ is the value of $V_{mes2}(\lambda)$ at 555 nm.

Fig. 5 plots the scotopic and photopic spectral luminous efficiency, and the mesopic spectral luminous efficiency functions for LEDs (CCTs are 3500 K, 4000 K, 4500 K, 5000 K, 5700 K, and 6500 K) for photopic luminance at 1 cd/m^2. It can be seen from figure that the difference is small between mesopic spectral luminous efficiency functions under different CCTs. And these mesopic spectral luminous efficiency functions (background luminance at 1 cd/m^2) are closer to photopic spectral luminous efficiency function.

Step 4: calculation of mesopic luminance L_{mes}.

The mesopic luminances under different S/P-ratios with four photopic background luminances (1 cd/m^2, 2 cd/m^2, 3 cd/m^2 and 4 cd/m^2) are presented in Table 3. It suggests that the mesopic luminances under different S/P-ratios are greater than the corresponding photopic luminance. When the L_p is constant, the mesopic luminance increases gradually from S/P-ratio = 1.598 to S/P-ratio = 2.269.

Fig. 6 plots the ratio of mesopic luminance to photopic luminance (L_{mes}/L_p) for L_p at 1 cd/m^2, 2 cd/m^2, 3 cd/m^2, and 4 cd/m^2 and CCT at 3500 K, 4000 K, 4500 K, 5000 K, 5700 K, and 6500 K.

Fig. 6 shows that the ratio of mesopic luminance to photopic luminance increased with the decreasing of photopic luminance within a certain LED CCT. And when the L_p is a constant,

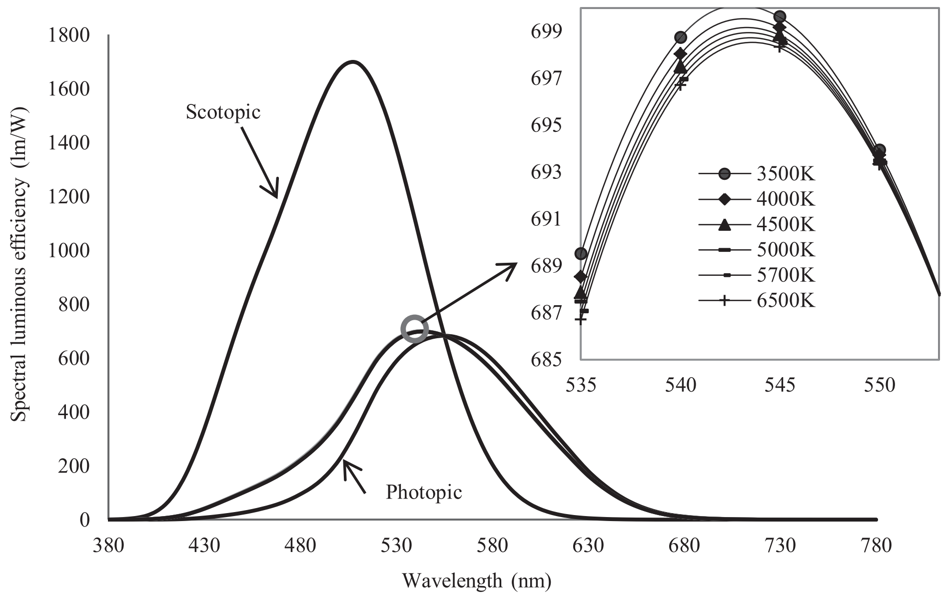

Fig. 5. The variation of m_2 with L_p and S/P-ratio.

TABLE 3
The Values of Mesopic Luminance Given by MES-2 Model Under Different S/P-Ratios With Four Photopic Luminances

L_{mes} / S/P-ratio	Photopic luminance (L_p) (cd/m^2)			
	1	2	3	4
1.598 (3500K)	1.0623	2.0666	3.0538	4.0305
1.817 (4000K)	1.0838	2.0897	3.0725	4.0412
1.977 (4500K)	1.0991	2.1063	3.0859	4.0488
2.074 (5000K)	1.1083	2.1161	3.0939	4.0534
2.178 (5700K)	1.1180	2.1266	3.1024	4.0582
2.269 (6500K)	1.1264	2.1356	3.1097	4.0624

L_{mes}/L_p had a great extent increase from 3500 K to 5000 K and become slowness from 5000 K to 6500 K. Besides, the values of L_{mes}/L_p of different CCTs have been slow to change in higher photopic luminance L_p (seen the bottom curve in Fig. 6).

4. Experimental Methodology

It can be seen from Section 3 that, although the photopic luminance measured by the luminance meter (which is only available in market and corrected by the photopic spectral luminous efficiency function V (λ)) is same, the eyes' perception luminance is different under various CCTs of light source, and the perception luminance is increasing with the increase of the LED CCT. In order to test the effect of CCTs on human visual performance, reaction times to different light source CCTs were determined at four mesopic luminance levels (1 cd/m^2, 2 cd/m^2, 3 cd/m^2, and 4 cd/m^2). Ten observers participated in. And there were 144 lighting conditions.

4.1 Observers

Ten Chinese observers (five females and five males) aged 22 to 26 participated in the experiment. They all have normal color vision in terms of the Ishihara test.

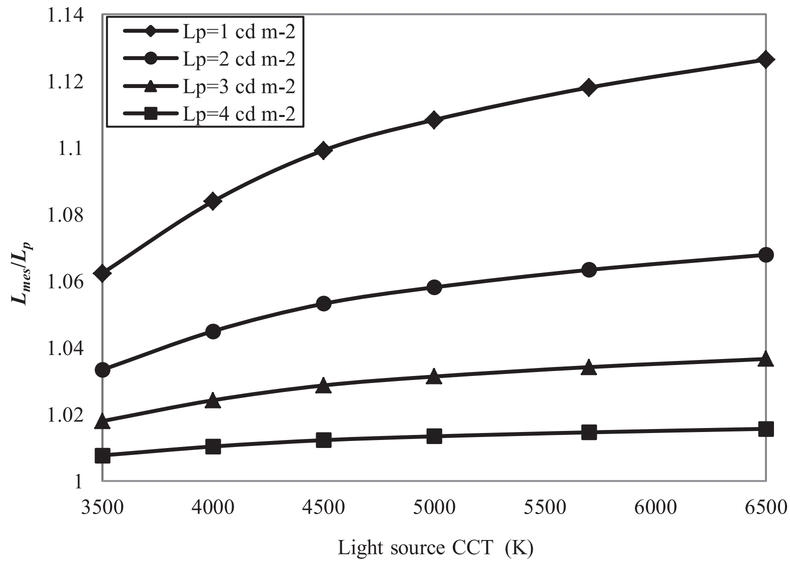

Fig. 6. The value of L_{mes}/L_p given by the MES-2 model.

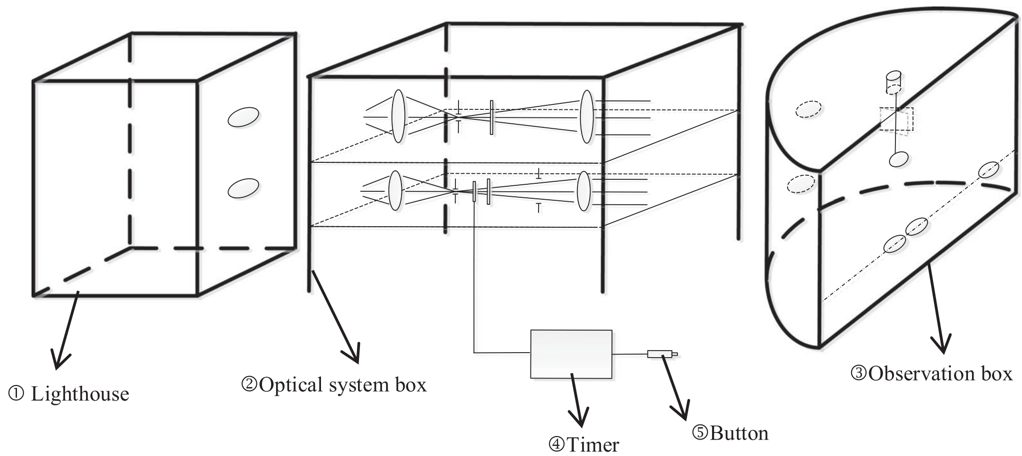

Fig. 7. The experimental set-up.

4.2 Experimental Set-Up

Fig. 7 illustrates a schematic diagram of experimental set-up. It consists of lighthouse, optical system box, and observation box. The LED light source is put in the lighthouse, which CCT and luminance can be adjusted as needed. Optical system box is divided into upper and lower layers. The upper layer provides the uniform background luminance for the experiment, and the lower gives luminance of the target light spot. The spectral of the background and target are nearly identical since the same light source is used for both. Besides, it also includes a timer, which can record the reaction time, which is the time interval between the appearance of the target and the push of the button by the observer [18]. Observer can see the background and target light spot in the observation box.

And the experiment equipment is shown in Fig. 8(a). Fig. 8(b) gives the viewing distance of the observers and the target size. Fig. 8(c) shows the experimental situation. This is implemented in a darkroom, avoiding the interference of the external luminance.

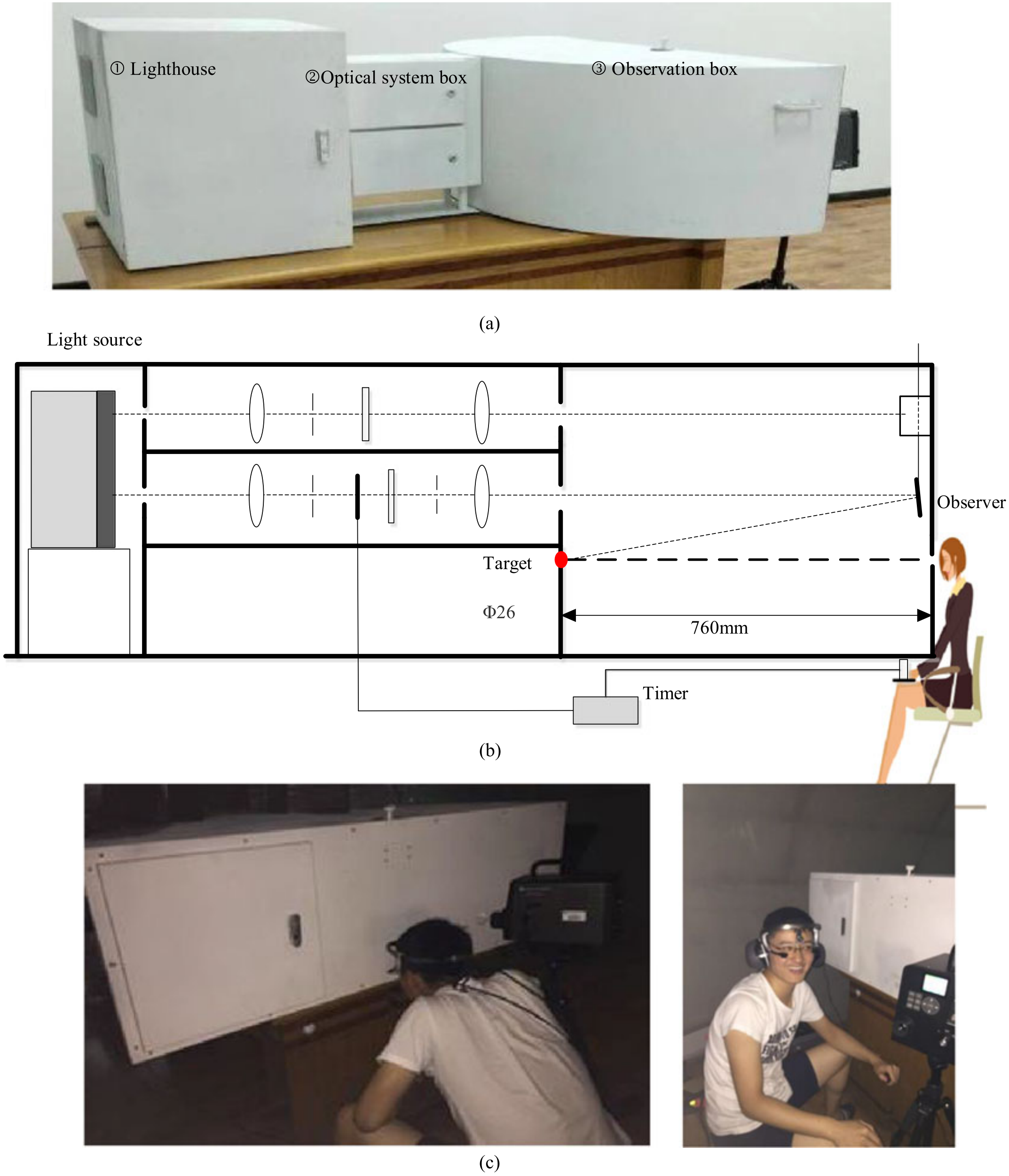

Fig. 8. The experimental situation.

Fig. 9. Components of the experimental set-up. (a) Lighthouse and light source. (b) Optical system and timer. (c) Observation box and spectrophotometer. (d) Situation seen by human eyes.

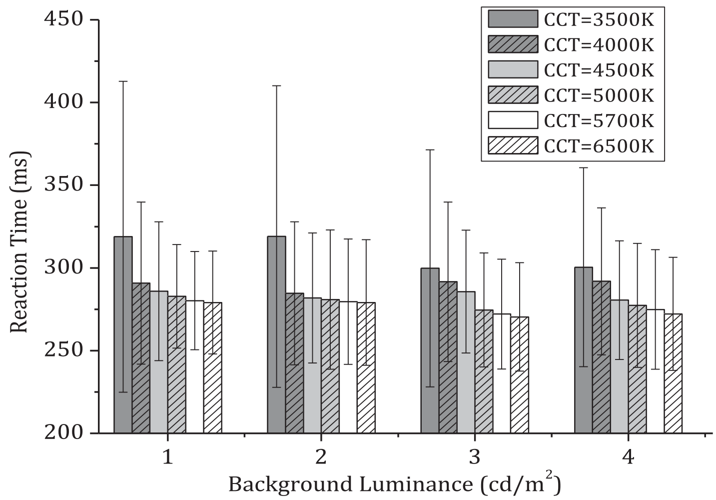

Fig. 10. Effect of CCT on mean reaction times for different background luminances. The error bars indicated the standard deviation.

Fig. 9 shows the components of the experimental set-up. Fig. 9(d) is the situation which is seen by human eyes. The bright spot is the target position.

4.3 Lighting

In total, there are 144 lighting conditions in the experiment, and the photometric data is shown in Table 4. Six CCTs (3500, 4000, 4500, 5000, 5700, and 6500 K), three Color Rendering Indexs (CRI, 65, 75, and 85, which are available CRI values of LEDs in market), four uniform background luminances (1, 2, 3, and 4 cd/m^2), two target contrasts (0.3 and 0.5), and two horizontal eccentricities ($\theta = 0°$ and $\theta = 5°$) are applied in the experiment. And the measured and target CCT have a difference under 40 K [19]. The target contrast can be calculated by the (8),

$$C = \frac{L_t - L_b}{L_b} \tag{8}$$

where C is the target contrast, L_b is the background luminance, and the L_t is the target luminance.

4.4 Procedure

Firstly, observers were tested for their color vision by the Ishihara test. And before starting the experiment, the observers were given 1 minute to adjust the background luminance. Each observer participated in six sessions. Each session consisted of 24 lighting conditions (one CCT, four background luminances, two target contrasts, three CRIs, two horizontal eccentricities). Under one lighting condition, the observer was asked to fix on the target position (which is marked with a cross by a pencil), and pressed the button when they detected the appearance of target light spot. The time interval between the appearance of the target and the push of the button by the observer was the reaction time under this lighting condition.

4.5 Results and Discussion

Fig. 10 shows the effect of CCT on reaction times averaged over all target contrasts, CRIs and eccentricities at background luminances 1, 2, 3, 4 cd/m^2.

It can be seen from Fig. 10 that, the mean reaction time decreases as CCT increases under all the background luminance. It has a function large decrease in lower CCT (from 3500 K to 4500 K),

TABLE 4
Parameters of 144 Lighting Conditions

No.	Target CCT (K)	Target L_b (cd/m^2)	C	Target θ	CRI	Target L_t (cd/m^2)	Measured CCT (K)	Measured L_b (cd/m^2)	Measured L_t (cd/m^2)
1	3500K	1	0.3	0°	/	1.3	3488	0.997	1.290
2				5°					
3			0.5	0°	65	1.5	3465	1.008	1.490
4					75		3500	0.978	1.477
5					85		3522	0.991	1.503
6				5°	/		3478	1.020	1.498
7		2	0.3	0°	/	2.6	3514	1.907	2.583
8				5°					
9			0.5	0°	65	3.0	3500	1.998	3.076
10					75		3529	2.012	2.972
11					85		3533	1.987	2.864
12				5°	/		3518	1.915	2.995
13		3	0.3	0°	/	3.9	3489	3.122	4.081
14				5°					
15			0.5	0°	65	4.5	3474	2.927	4.447
16					75		3531	2.994	4.508
17					85		3490	3.104	4.531
18				5°	/		3487	2.872	4.603
19		4	0.3	0°	/	5.2	3510	4.144	5.192
20				5°					
21			0.5	0°	65	6.0	3496	3.975	5.957
22					75		3536	3.893	5.971
23					85		3526	4.142	6.097
24				5°	/		3534	3.907	6.112
25	4000K	1	0.3	0°	/	1.3	3975	1.098	1.291
26				5°					
27			0.5	0°	65	1.5	3963	1.128	1.494
28					75		3976	0.953	1.445
29					85		4000	0.948	1.579
30				5°	/		4026	1.044	1.509
31		2	0.3	0°	/	2.6	4019	1.942	2.632
32				5°					
33			0.5	0°	65	3.0	3982	1.980	2.945
34					75		3978	2.052	3.172
35					85		4019	2.187	3.016
36				5°	/		4031	2.026	3.045
37		3	0.3	0°	/	3.9	4035	2.921	3.906
38				5°					
39			0.5	0°	65	4.5	3999	3.007	4.557
40					75		4035	3.058	4.546
41					85		4018	2.941	4.613
42				5°	/		4023	2.896	4.473
43		4	0.3	0°	/	5.2	4021	3.922	5.282
44				5°					

No.	Target CCT (K)	Target L_b (cd/m^2)	C	Target θ	CRI	Target L_t (cd/m^2)	Measured CCT (K)	Measured L_b (cd/m^2)	Measured L_t (cd/m^2)
45			0.5	0°	65	6.0	4022	3.876	6.016
46					75		4037	4.123	6.129
47					85		3994	4.076	5.928
48				5°	/		3986	3.932	5.906
49	4500K	1	0.3	0°	/	1.3	4511	0.931	1.305
50				5°					
51			0.5	0°	65	1.5	4537	1.008	1.492
52					75		4518	0.932	1.431
53					85		4504	1.132	1.385
54				5°	/		4498	0.872	1.483
55		2	0.3	0°	/	2.6	4539	2.117	2.546
56				5°					
57			0.5	0°	65	3.0	4472	2.016	2.856
58					75		4535	1.920	3.107
59					85		4486	1.883	3.162
60				5°	/		4509	2.057	3.005
61		3	0.3	0°	/	3.9	4532	3.014	3.921
62				5°					
63			0.5	0°	65	4.5	4515	2.873	4.470
64					75		4489	2.922	4.433
65					85		4468	2.970	4.602
66				5°	/		4540	3.005	4.504
67		4	0.3	0°	/	5.2	4523	3.900	5.204
68				5°					
69			0.5	0°	65	6.0	4470	4.012	5.945
70					75		4527	4.190	6.124
71					85		4520	3.980	6.045
72				5°	/		4491	3.941	5.980
73	5000K	1	0.3	0°	/	1.3	4989	1.044	1.308
74				5°					
75			0.5	0°	65	1.5	5026	0.936	1.608
76					75		5019	1.061	1.483
77					85		5037	1.153	1.432
78				5°	/		4992	0.889	1.482
79		2	0.3	0°	/	2.6	5021	1.891	2.604
80				5°					
81			0.5	0°	65	3.0	4971	2.043	3.061
82					75		4981	2.137	2.974
83					85		5010	1.937	2.886
84				5°	/		5018	1.873	2.951
85		3	0.3	0°	/	3.9	5024	2.896	3.904
86				5°					
87			0.5	0°	65	4.5	4986	2.953	4.579
88					75		4990	3.118	4.585
89					85		5024	2.958	4.609
90				5°	/		5038	3.034	4.603
91		4	0.3	0°	/	5.2	4989	3.972	5.310
92				5°					
93			0.5	0°	65	6.0	4964	4.039	6.112
94					75		4986	4.060	5.877
95					85		5027	3.999	5.949
96				5°	/		4988	3.880	6.127

No.	Target CCT (K)	Target L_b (cd/m^2)	C	Target θ	CRI	Target L_t (cd/m^2)	Measured CCT (K)	Measured L_b (cd/m^2)	Measured L_t (cd/m^2)
97	5700K	1	0.3	0°	/	1.3	5735	0.986	1.302
98				5°					
99			0.5	0°	65	1.5	5671	1.012	1.470
100					75		5692	0.873	1.508
101					85		5693	1.147	1.492
102				5°	/		5723	0.917	1.516
103		2	0.3	0°	/	2.6	5687	2.107	2.601
104				5°					
105			0.5	0°	65	3.0	5672	1.890	3.001
106					75		5737	1.941	2.881
107					85		5697	2.122	2.952
108				5°	/		5673	2.181	3.051
109		3	0.3	0°	/	3.9	5724	2.971	3.903
110				5°					
111			0.5	0°	65	4.5	5707	3.056	4.580
112					75		4983	3.105	4.642
113					85		5702	2.875	4.389
114				5°	/		5731	3.123	4.612
115		4	0.3	0°	/	5.2	5684	4.082	5.205
116				5°					
117			0.5	0°	65	6.0	5739	4.004	6.091
118					75		5724	3.874	6.163
119					85		5718	3.945	5.897
120				5°	/		5692	4.074	5.949
121	6500K	1	0.3	0°	/	1.3	6522	0.949	1.290
122				5°					
123			0.5	0°	65	1.5	6502	0.936	1.486
124					75		6498	1.127	1.508
125					85		6471	1.003	1.490
126				5°	/		6499	0.879	1.501
127		2	0.3	0°	/	2.6	6474	2.013	2.612
128				5°					
129			0.5	0°	65	3.0	6483	2.061	2.963
130					75		6467	1.991	3.006
131					85		6500	2.107	3.077
132				5°	/		6520	1.973	2.928
133		3	0.3	0°	/	3.9	6535	2.902	3.910
134				5°					
135			0.5	0°	65	4.5	6522	3.109	4.491
136					75		6513	3.094	4.613
137					85		6479	2.886	4.534
138				5°	/		6503	2.937	4.503
139		4	0.3	0°	/	5.2	6524	4.004	5.207
140				5°					
141			0.5	0°	65	6.0	6516	3.958	6.042
142					75		6474	4.026	5.939
143					85		6490	4.139	6.104
144				5°	/		6527	4.080	5.950

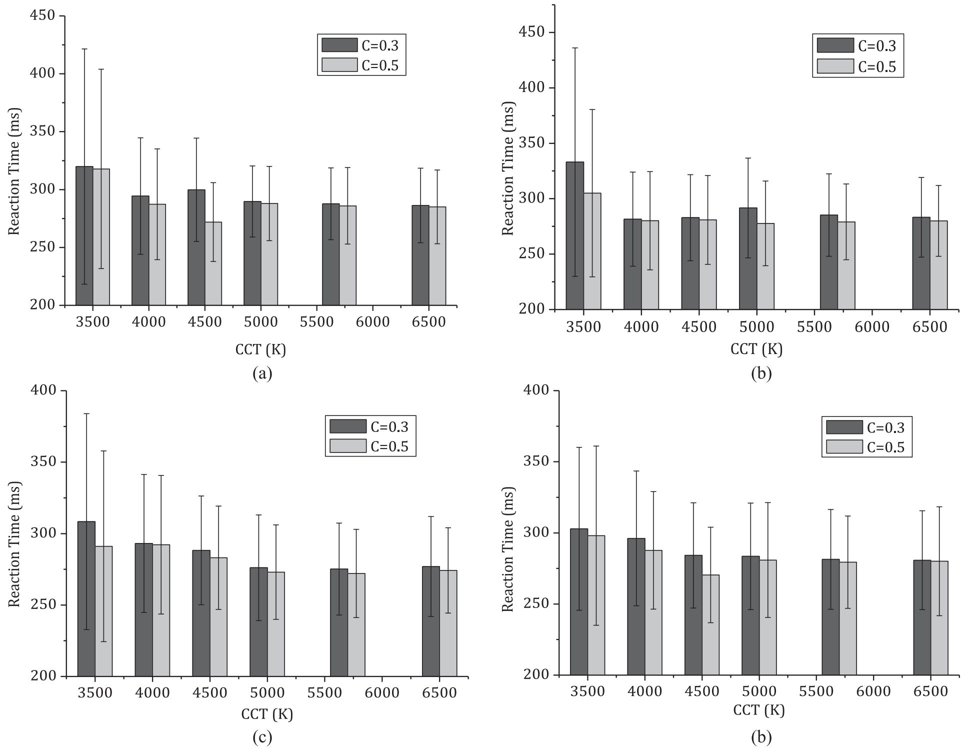

Fig. 11. Effect of contrast on mean reaction times for different background luminances. The error bars indicated the standard deviation. C = contrast. (a) $L_b = 1$ cd/m^2. (b) $L_b = 2$ cd/m^2. (c) $L_b = 3$ cd/m^2. (d) $L_b = 4$ cd/m^2.

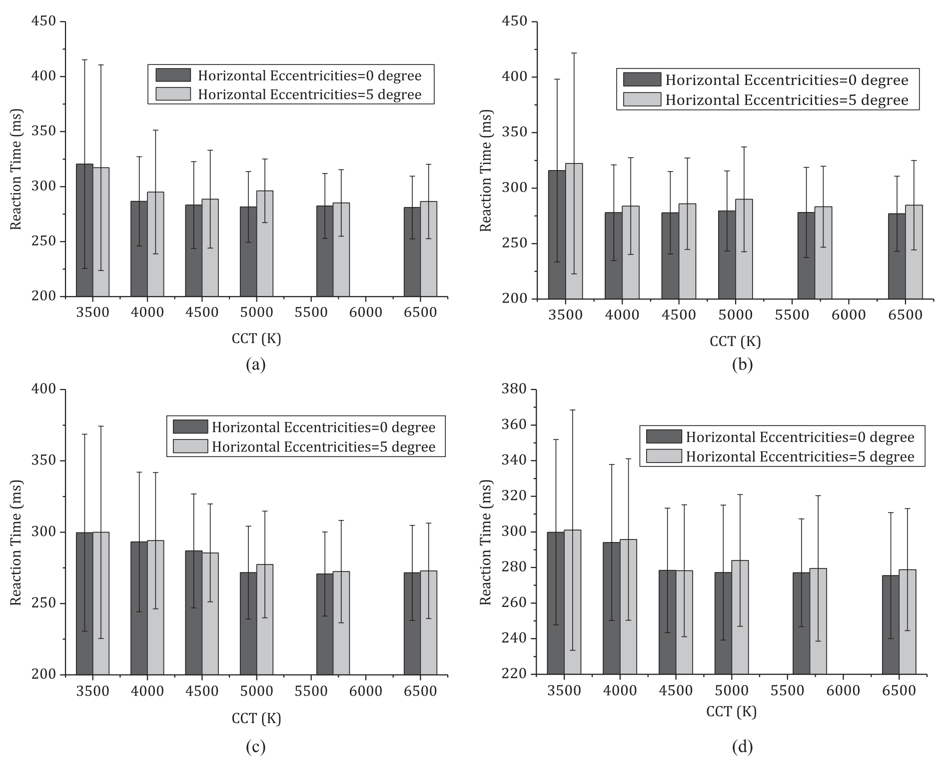

Fig. 12. Effect of horizontal eccentricities on mean reaction times for different background luminances. The error bars indicated the standard deviation. (a) $L_b = 1$ cd/m^2. (b) $L_b = 2$ cd/m^2. (c) $L_b = 3$ cd/m^2. (d) $L_b = 4$ cd/m^2.

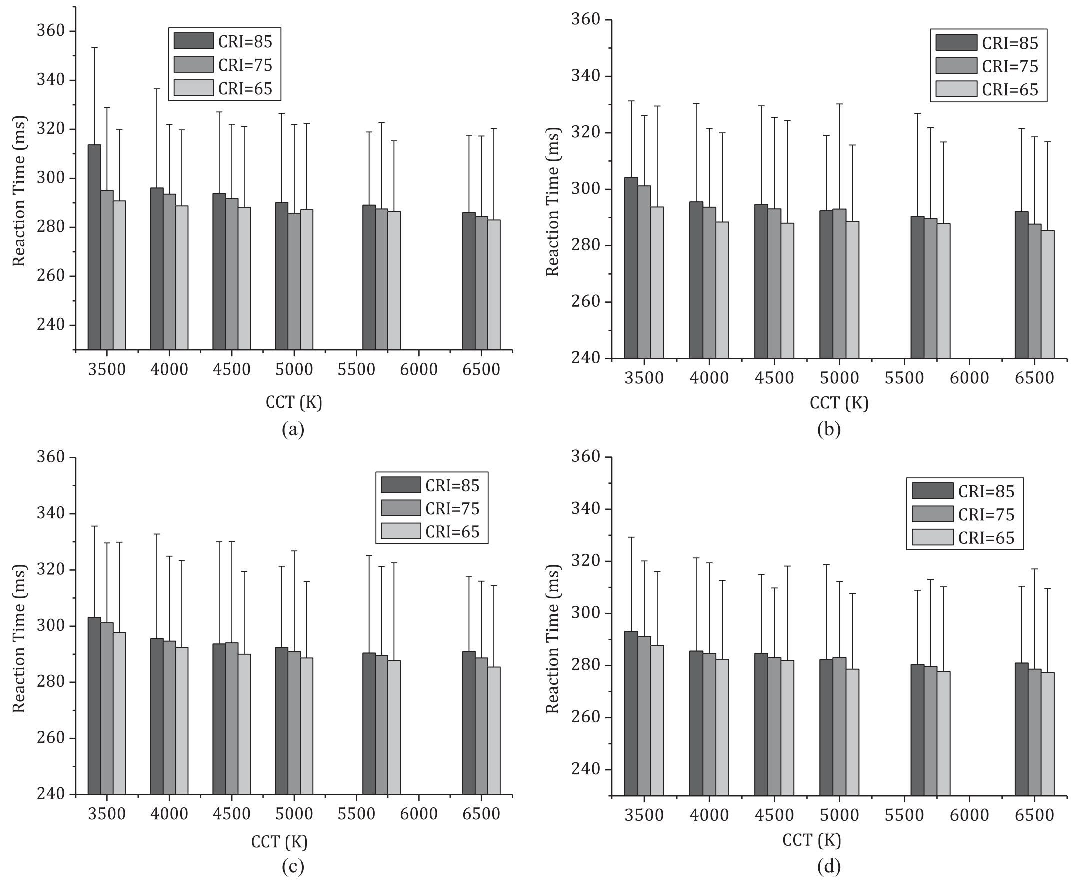

Fig. 13. Effect of CRI on mean reaction times for different background luminances. The error bars indicated the standard deviation. (a) $L_b = 1$ cd/m2, $C = 0.5$, $\theta = 0°$. (b) $L_b = 2$ cd/m^2, $C = 0.5$, $\theta = 0°$. (c) $L_b = 3$ cd/m^2, $C = 0.5$, $\theta = 0°$. (d) $L_b = 4$ cd/m^2, $C = 0.5$, $\theta = 0°$.

and shows a small decrease in the higher CCT (from 5000 K to 6500 K). The experiment results also agree with the above theoretical results.

Fig. 11 gives the effect of contrast on reaction times to different CCTs at different background luminance.

We can see from Fig. 11 that the mean reaction times for targets with 0.5 contrast were lower than those with 0.3 contrast. This indicates that observers are easier to make response at a high target contrast.

Fig. 12 shows the effect of horizontal eccentricities on mean reaction times to different CCTs at different background luminances. Reaction times to peripheral stimuli are slightly higher than fovea vision to different CCTs. And the difference in mean reaction times is significant at 5000 K compared to that at other CCTs.

Fig. 13 shows the effect of CRI (Color Rending Index) on mean reaction times to different CCTs at different background luminances. We can see from Fig. 13 that the mean reaction times are decreasing with the decrease of CRI. It means that the lower CRI can make human easy to identify the obstacle in mesopic luminance.

5. Conclusion

In this paper, a theoretical analysis and experiment were carried out to investigate the impact of LED lighting parameters of CCT under mesopic light levels on visual performance. Firstly, the mesopic spectral luminous efficiency $V_{mes}(\lambda)$ and mesopic luminance under different CCTs (with different

S/P-ratios) are analyzed based on the mesopic model MES-2 (which was recommended by CIE in 2010). It was found that though the photopic luminance measured by the luminance meter (which is only available in market) is same, the eyes' perception luminance is different under various CCTs of light source in mesopic region, and the perception luminance is increasing with the increase of the LED CCT, but tends to show a smaller increase in the higher CCT.

Then an experiment was used to measure the reaction time of human eye under different lighting conditions (6-CCTs, 3-CRIs, 4-background luminances, 2-contrasts, and 2-horizontal eccentricities). Results showed that the reaction time decreased with the increasing of CCTs, and showed a small decrease in the higher CCT. The experiment results also agree with the above theoretical results.

References

[1] J. C. Shin, H. Yaguchi, and S. Shioiri, "Change of color appearance in photopic, mesopic and scotopic vision," *Opt. Rev.*, vol. 11, no. 4, pp. 265–271, 2004.
[2] M. S. Islam, R. Dangol, M. Hyvärinen, P. Bhusal, M. Puolakka, and L. Halonen, "User acceptance studies for led office lighting: Lamp spectrum, spatial brightness and Illuminance," *Lighting Res. Technol.*, vol. 47, no. 1, pp. 54–79, 2013.
[3] Y. He, Z. Lang, A. Wu, and C. Li, "Research on intelligent control of tunnel lighting system based on LED," in *Proc. 2010 Int. Conf. Optoelectron. Image Process.*, Haikou, China, 2010, pp. 247–250.
[4] B. Mao, P. Niu, and C. Huang, "The design of the drive control chip for the solar LED lighting system," *Mod. Appl. Sci.*, vol. 2, no. 3, pp. 75–80, 2008.
[5] M. Viikari, W. Chen, M. Eloholma, L. Halonen, and D. Chen, "Comparative study of two visual performance based mesopic models based on reaction time and contrast threshold data," *Lighting Eng.*, vol. 4, no. 14, pp. 21–32, 2006.
[6] Commission Internationalede L'Eclairage, "Principales decisions (6e Session, 1924), CIE Sixie 'me Session, Gene've, Juillet, 1924. Recueil des Travaux et Compte Rendu de Se ´ances," pp. 67–69, 1926.
[7] M. Viikari, A. Ekrias, M. Eloholma, and L. Halonen, "Modeling spectral sensitivity at low light levels based on mesopic visual performance," *Clin. Ophthalmol.*, vol. 2, no. 1, pp. 173–85, 2008.
[8] H. V. Walters and W. D. Wright, "The spectral sensitivity of the fovea and extra fovea in the Purkinje range," *Proc. Roy. Soc. London B*, vol. 131, pp. 340–361, 1942.
[9] J. A. S. Kinney, "Effect of field size and position on mesopic spectral sensitivity," *J. Opt. Soc. Amer.*, vol. 54, pp. 671–677, 1964.
[10] Commission Internationalede L'Eclairage, "Mesopic photometry: History, special problems and practical solutions," CIE publication 81-1989, Vienna, Austria, 1989.
[11] Commission Internationalede L'Eclairage, "Testing of supplementary systems of photometry," CIE publication 141-2001, Vienna, Austria, 2001.
[12] M. S. Rea, J. D. Bullough, J. P. Freyssinier-Nova, and A. Bierman, "A proposed unified system of photometry," *Lighting Res. Technol.*, vol. 36, no. 2, pp. 85–111, 2004.
[13] Y. He, A. Bierman, and M. Rea, "A system of mesopic photometry," *Lighting Res. Technol.*, vol. 30, pp. 175–81, 1998.
[14] Y. He *et al.*, "Evaluating light source efficacy under mesopic conditions using reaction times," *J. Illum. Eng. Soc.*, vol. 26, pp. 125–38, 1997.
[15] M. Eloholma and L. Halonen, "New model for mesopic photometry and its application to road lighting," *LEUKOS*, vol. 2, no. 4, pp. 263–93, 2006.
[16] Commission Internationale de l'Eclairage, "Recommended system for mesopic photometry based on visual performance," CIE publication 191-2010, Vienna, Austria, 2010.
[17] A. Žukauskas, R. Vaicekauskas, A. Tuzikas, and A. Petrulis, "Firelight led source: Toward a balanced approach to the performance of solid-state lighting for outdoor environments," *IEEE Photon. J.*, vol. 6, no. 3, pp. 1–16, Jun. 2014, Art. no. 8200316.
[18] M. Rea, "Evaluating light source efficacy under mesopic conditions using reaction times," *J. Illum. Eng. Soc.*, vol. 26, no. 1, pp. 125–138, 1997.
[19] H. Jin, S. Jin, L. Chen, S. Cen, and K. Yuan, "Research on the lighting performance of led street lights with different color temperatures," *IEEE Photon. J.*, vol. 7, no. 6, Dec. 2015, Art. no. 1601309.